

# Numerical study of Lyapunov exponents for products of correlated random matrices

Hiroaki Yamada\*

*Department of Material Science and Technology, Faculty of Engineering, Niigata University, Ikarashi 2-Nocho 8050, Niigata 950-2181, Japan*

Tsuneyasu Okabe†

*Japan Science and Technology Corporation, National Institute of Materials and Chemical Research, Higashi 1-1, Tukuba, 305-8565, Japan*

(Received 9 May 2000; revised manuscript received 28 August 2000; published 18 January 2001)

We numerically study Lyapunov spectra and the maximal Lyapunov exponent (MLE) in products of real symplectic correlated random matrices, each of which is generated by a modified Bernoulli map. We can systematically investigate the influence of the correlation on the Lyapunov exponents because the statistical properties of the sequence generated by the map, whose correlation function shows power-law decay, have been well investigated. It is shown that the form of the scaled Lyapunov spectra does not change much even if the correlation of the sequence increases in the stationary region, and in the nonstationary region the forms are quite different from those obtained in the  $\delta$ -correlated purely random case. The fluctuation strength dependence of the MLE changes with increasing correlation, and a different scaling law from that of the  $\delta$ -correlated case can be observed in the nonstationary region. Moreover, the statistical properties of the probability distribution of the local Lyapunov exponents are quite different from those obtained from  $\delta$ -correlated random matrices. Slower convergence that does not obey the central-limit theorem is observed for increasing correlation.

DOI: 10.1103/PhysRevE.63.026203

PACS number(s): 05.45.-a, 05.40.-a, 72.15.Rn, 02.30.Xx

## I. INTRODUCTION

Many physical problems are related to the study of the asymptotic behavior of products of random matrices (PRMs) [1–3]. Examples are localization of lattices vibration in disordered lattices [4–6], localization of quantum particles in disordered systems [5,7,8], the random Ising model of ferromagnetic materials [9,10], instability of dynamical systems [11–19], and the problem of directed polymers in a random medium [20].

Some mathematicians have given rigorous results for PRMs. The pioneering work of Furstenberg gives a law of large numbers of matrices belonging to noncompact semisimple Lie groups [21]. Oseledec proved a multiplicative ergodic theorem that ensures the existence of the Lyapunov exponents in independent identically distributed (i.i.d.) random symplectic matrices [22]. Tutubalin showed that the asymptotic probability distribution  $P_m(R)$  of  $\delta$ -correlated PRMs of unitary group for large  $m$ , where  $R = M_m M_{m-1} \cdots M_2 M_1$  are PRMs, converges to a Gaussian distribution [23]. Virster generalized the results obtained by Tutubalin to arbitrary groups with noncompact connected semisimple Lie groups, such as  $SU(N, N)$  [24]. These theorems correspond to the central-limit theorem (CLT) in PRMs. The CLT on the group  $SU(N, N)$ , which shows the existence of the probability distribution  $P_m(R)$  in the large  $m$  limit, has been given by some authors [25–27]. Newman was able to

give a closed expression for all the Lyapunov exponents when the matrix elements were distributed according to a Gaussian distribution, for large  $N \times N$  matrix products [28,29].

Physicists have carefully applied these mathematical results to some physics problems. Matsuda and Ishii related Furstenberg's theorem to localization problems in one-dimensional disordered systems [4]. Kissel [30] derived the Lyapunov exponents in multichannel localization as a function of the transmission matrix by using the Oseledec theorem [22]. O'Connor proved the CLT for the amplitudes of plane waves traveling in a semi-infinite isotropic disordered harmonic chain, and it has been applied to the problem of heat conduction in disordered harmonic chains [26]. In all the cases mentioned above, products of independently distributed matrices, i.e.,  $\delta$ -correlated matrices, were dealt with. However, the asymptotic properties for correlated PRMs are also interesting problems in physics. We will investigate properties of correlated PRMs in the present paper.

In classical dynamical systems with many degrees of freedom, the instability of the tangent vector of the trajectories plays an important role when we consider the statistical mechanics of the system. Lyapunov exponents, which are the exponential growth of the vectors along the trajectories, can be numerically estimated from products of real symplectic matrices, and the statistical properties of the Lyapunov exponents depend on the statistical properties of the time series of the fluctuation of the matrix elements [3,28]. Moreover, it is well known that  $1/f$  type fluctuation in the power spectrum, corresponding to the existence of long-time correlation, is observed in the time dependence of some physical quantities, such as the total and one-particle potential energy, in many kinds of dynamical systems. For example, Fukamachi showed the  $1/f$  type fluctuation of the FPU model [31].

\*Electronic address: hyamada@cc.niigata-u.ac.jp

†Present address: Language Institute, The University of Waikato, P.O. Box 1317, Waikato Mail Center, Hamilton, New Zealand. Electronic address: okabe@tsphys.eng.niigata-u.ac.jp

Okabe and Yamada also observed a similar fluctuation in a one-dimensional Lennard-Jones system [32]. These results show that a variety of dynamical behaviors can be observed in a dynamical system due to correlation that is different from  $\delta$ -correlated motion in random processes. Correlation effects in some dynamical systems have also been reported in different contexts [33–35]. Some authors have pointed out the importance of correlation effects of dynamical systems for Lyapunov spectra and the scaling form of the maximal Lyapunov exponent, in comparison with  $\delta$ -correlated random matrix products.

However, the statistical properties of the products of correlated random matrices have not been studied, except for a few numerical studies [36–38,41]. Crisanti *et al.* investigated the correlation effects on dynamical instability and showed a discrepancy between the dynamical system and the random matrix approximation (RMA) due to correlation in low-dimensional maps [16,3]. Yamada *et al.* have shown for products of  $2 \times 2$  matrices that the convergent properties of the probability distribution of the transmission rate with respect to the system size do not obey the CLT; they have slower convergence because of the correlation of the sequence, in the context of a one-dimensional disordered system with long-range structural correlation [36]. Oliver and Petri gave exact expressions for the Lyapunov exponents of correlated PRMs with Markovian rules [38]. It is worth noting that a one-dimensional disordered system with off-diagonal randomness can be expressed by PRMs with Markovian rules. Goda showed analytically that Furstenberg’s convergence theorem is applicable to this case [39].

Moreover, it has been detected that the matrix elements show a certain degree of correlation in the fluctuation of the time evolution in some dynamical systems [32,40]. Accordingly, to investigate systematically the effect of correlation on some statistical properties of the PRMs may give useful information for dynamical systems. Yamaguchi investigated the effects of exponential correlation on the shape of Lyapunov spectra by changing the correlation length in one-dimensional nonlinear chains [41]. It has been shown that exponential correlation changes the shape of the Lyapunov spectra from linear to curved. Okabe and Yamada gave a preliminary report on correlation effects on Lyapunov spectra and the scaling form of the maximal Lyapunov exponent (MLE) [42] where the correlated sequences are generated by a modified Bernoulli map (see below).

In this paper, we study numerically some asymptotic properties of Lyapunov exponents in products of symplectic random matrices with long-range correlation, each of which is produced by a modified Bernoulli map [43–45]. We give results by more systematic investigation for wider ranges of parameters than in our preliminary report [42]. The modified Bernoulli map generates correlated sequences in which the correlation function decays obeying an inverse power law, i.e., the correlation length is infinite. The statistical properties of the sequence of the modified Bernoulli map have been well studied by Aizawa *et al.* [43,44], who used the map in order to reveal the statistical properties of intermittent chaos. Thus we can systematically investigate the influence of correlation on the Lyapunov spectra, the scaling form of the

TABLE I. The classification of cases by combination of three matrix forms and two symbolic types that we use in the present paper.

Form	A	B	C
Type 1 (0 or $\epsilon$ )	case A1	case B1	case C1
Type 2 ( $-\epsilon/2$ or $\epsilon/2$ )	case A2	case B2	case C2

MLE, and the statistical properties of the probability distribution of local Lyapunov exponents [42].

We found some interesting results for the correlation effect on Lyapunov exponents. For example, in dynamical models, with increase of correlation all the Lyapunov exponents increase in the stationary region. On the other hand, in the nonstationary region the MLE increases with increase of the correlation, but the smaller Lyapunov exponents begin to decrease. Moreover, we observed a clear scaling law for the maximal Lyapunov exponent,  $\lambda_1(\epsilon) \sim \epsilon^\beta$ , where depending on the correlation the exponent  $\beta$  takes intermediate values between  $2/3$  and  $1/2$  in the stationary region. In the nonstationary region, however, the correlation does not greatly affect the scaling form of the MLE  $\lambda_1$ . In comparison with the RMA, the slower convergent properties of the probability distribution with respect to time are well observed. The details of the numerical results are given in the present paper.

This paper is constructed as follows. In the next section, we introduce three kinds of the symplectic matrix form we use. Two of them are based on interacting classical particles in one dimension. We refer to them as form A and form B. In the text of this paper we mainly focus on form A. The case for form B is mainly shown in Sec. VIII. We also give results for another matrix form (form C) based on localization in quasi-one-dimensional disordered systems in Sec. VIII.

In Sec. III, we introduce the modified Bernoulli map that generates the correlated sequence. We mainly use two types of symbolic sequence which take only two values 0 or  $\epsilon$  (type 1) and  $-\epsilon/2$  or  $\epsilon/2$  (type 2), where  $\epsilon$  means the strength of the fluctuation. We investigate some properties of the Lyapunov exponents for some cases by changing the combination of the above three kinds of matrix form and two kinds of distribution. (See Table I.)

In Sec. IV, we give a definition and brief explanation of the Lyapunov exponents and local Lyapunov exponents we used in this paper. We give numerical results for the matrix form A in Secs. V, VI, and VII.

In Sec. V, we investigate the Lyapunov spectra for matrix form A with two kinds of probability distribution. It has been shown that scaled Lyapunov spectra  $L_S(x)$ ,  $x = i/N$ , become linear, i.e.,  $L_S(x) \propto 1 - x$ , in the limit  $N \rightarrow \infty$  in the case of PRMs with no correlation or a strongly chaotic regime [3]. In the stationary region, the form of the Lyapunov spectra does not greatly depend on the strength of the correlation and the dependence is quasilinear. It will be shown that in the nonstationary region the forms of Lyapunov spectra become curved, depending on the strength of the correlation.

In Sec. VI, we investigate the dependence of the MLE on the  $\lambda_1(\epsilon)$ , fluctuation strength  $\epsilon$ , for various cases of combination of the matrix form and symbolized type. In the

RMA  $\lambda_1(\epsilon) \sim \epsilon^{2/3}$  is shown in the weak disorder limit by using analytical methods, such as the weak disorder expansion and replica trick and so on [3]. We showed that the scaling form  $\lambda_1(\epsilon)$  becomes different from that in the RMA in the nonsymbolic model in which the sequence takes values in the interval  $[0, \epsilon]$  or  $[-\epsilon/2, \epsilon/2]$  in our preliminary report [42]. We show some interesting scaling forms  $\lambda_1(\epsilon)$  for the discretized (two-value) version in the present paper.

In Sec. VII, the statistical properties of the probability distribution of the local MLE are investigated. Section VIII contains some numerical results in the other cases of matrix forms B and C. The last section is devoted to summary and discussion.

## II. MATRIX FORMS

In this section, we introduce the matrix forms and some terminology we use hereafter, based on Hamiltonian dynamical systems. Although we do not treat the Hamiltonian system itself in the present paper, this is convenient for readers when they consider the background of this problem.

We consider a one-dimensional classical many-body system with  $N$  degrees of freedom in order to set the matrix form, in which the  $2N$ -dimensional phase space consists of generalized coordinates and momenta  $(p_1, \dots, p_N, q_1, \dots, q_N)$ . In general, the Hamiltonian  $H = \sum_{i=1}^N p_i^2/2 + U_{tot}(q_1, \dots, q_N)$  describes a one-dimensional system obeying classical dynamics. In the Hamilton system,

Lyapunov exponents, which are indices of instability of the trajectory in phase space, can be calculated by the time evolution of an infinitesimally perturbed vector  $\delta\mathbf{z}(t) = (\delta p_1(t), \dots, \delta p_N(t), \delta q_1(t), \dots, \delta q_N(t))$  in  $2N$ -dimensional tangent space [3,46,47]. The discrete time evolution of the system is given by

$$\mathbf{Z}(t=n\delta t) = \prod_{i=1}^n \mathbf{S}^{(i)} \mathbf{Z}(0) \equiv \mathbf{P}(t) \mathbf{Z}(0), \quad (2.1)$$

where the matrix  $\mathbf{S}^{(i)}$  is a real symplectic Jacobian matrix for  $\delta t$  time evolution and  $\mathbf{Z}(0)$  is a  $2N$ -dimensional arbitrary real orthogonal matrix. The matrix can be determined only by coordinates  $\mathbf{q}(t)$  obtained as the solution of the equation of motion. Then the form of the symplectic matrices is [3]

$$\mathbf{S}^{(i)} = \begin{pmatrix} \mathbf{I} & \delta t \mathbf{I} \\ -\delta t \mathbf{H}^{(i)} & \mathbf{I} - \delta t^2 \mathbf{H}^{(i)} \end{pmatrix}, \quad (2.2)$$

where  $\mathbf{I}$  and  $\mathbf{H}^{(i)}$  are  $N$ -dimensional unit and real symmetric (Hessian) matrices, respectively. First, we adopt the Hessian matrix of a one-dimensional dynamical system with nearest-neighbor interaction and periodic boundary conditions as the matrix form of  $\mathbf{H}^{(i)}$ . Accordingly, the sum of each row must be zero, and so is that of each column,  $\sum_{l=1}^N \mathbf{H}^{(i)}_{lk} = 0$ ,  $k = 1, \dots, N$ , based on the conservation of the momentum. As a result, the matrix form of  $\mathbf{H}^{(i)}$  becomes tridiagonal with two corner elements as follows:

$$\mathbf{H}^{(i)} = \begin{pmatrix} \omega_{N1} + \omega_{12} & -\omega_{12} & 0 & \cdots & 0 & -\omega_{1N} \\ -\omega_{12} & \omega_{12} + \omega_{23} & -\omega_{23} & 0 & \ddots & 0 \\ 0 & -\omega_{23} & \omega_{23} + \omega_{34} & \ddots & \ddots & \vdots \\ \vdots & \ddots & \ddots & \ddots & \ddots & 0 \\ 0 & \ddots & \ddots & \ddots & \ddots & -\omega_{N-1N} \\ -\omega_{1N} & 0 & \cdots & 0 & -\omega_{N-1N} & \omega_{N-1N} + \omega_{N1} \end{pmatrix}, \quad (2.3)$$

where the  $\{\mathbf{H}_{ij}\}$  are given by second partial derivatives of the total potential energy,

$$\omega_{ii+1} = -\frac{\partial^2 U_{tot}(q_1, \dots, q_N)}{\partial q_i \partial q_{i+1}}. \quad (2.4)$$

See Refs. [47,32] for details.

In the RMA matrix elements  $\{\omega_{jj+1}\}$ 's are i.i.d. random variables with an appropriate density function, such as uniform distribution in an interval  $[-\epsilon/2, \epsilon/2]$ .  $\epsilon$  is a parameter that controls the strength of the fluctuation (or randomness). Moreover, we consider another case in which the diagonal elements are positive definite values, which corresponds to a typical high energy state in a one-dimensional dynamical system. Indeed, we used a distribution range  $[0, \epsilon]$  in our

previous report [42]. As we noted in Sec. I, here we deal with two types of a symbolic distribution that takes two values. (See Sec. III.)

Before closing this section let us introduce other matrix forms which were not investigated in [42]. One of them is a case in which all of the matrix elements of the Hessian are random variables. Then the number of independent random variables becomes  $N(N+1)/2$  because of the symmetry. This corresponds, for example, to a one-dimensional dynamical system with interaction between all particles, such as a coupled map system with cosine potential except in the conservation law [48,33]. We refer to this form of the Hessian matrix as form B and deal with it in Sec. VIII.

Another matrix form comes from the tight binding model of a quasi one-dimensional disordered system. The Schrödinger equation of the system is  $\Psi_{nm+1} + \Psi_{nm-1} + \Psi_{n-1m} + \Psi_{n+1m} + V_{nm} \Psi_{nm} = E \Psi_{nm}$ , where  $\Psi_{nm}$ ,  $V_{nm}$ , and  $E$  are

the wave function, the potential on the site  $(n, m)$ , and the energy of the system. The equation can be written in recursive form,

$$\mathbf{Z}(n) = \prod_{i=1}^n \mathbf{S}^{(i)} \mathbf{Z}(0) \equiv \mathbf{P}(n) \mathbf{Z}(0), \quad (2.5)$$

where  $(\mathbf{Z}(n))^t = (\Psi_{n1}, \dots, \Psi_{nN}, \Psi_{n-11}, \dots, \Psi_{n-1N})$ . In periodic boundary conditions the matrix form  $\mathbf{S}^{(i)}$  is given as

$$\mathbf{S}^{(i)} = \begin{pmatrix} E\mathbf{I} - \mathbf{H}^{(i)} & -\mathbf{I} \\ \mathbf{I} & \mathbf{0} \end{pmatrix}, \quad (2.6)$$

where  $\mathbf{0}$  is an  $N$ -dimensional null matrix.  $E$  denotes the energy of an electron injected into the system from a perfect conductor on the left side, and  $\mathbf{H}^{(i)}$  is the Hamiltonian of the  $i$ th slice of the two-dimensional strip. The matrix form of  $\mathbf{H}^{(i)}$  becomes tridiagonal with two corner elements as follows:

$$\mathbf{H}^{(i)} = \begin{pmatrix} V_{i1} & 1 & 0 & \cdots & 0 & 1 \\ 1 & V_{i2} & 1 & 0 & \cdots & 0 \\ 0 & 1 & V_{i3} & 1 & \cdots & 0 \\ \vdots & \vdots & \ddots & \ddots & \ddots & \ddots \\ 1 & 0 & 0 & \cdots & 1 & V_{iN} \end{pmatrix}. \quad (2.7)$$

In this case the number of random variables is  $N$ , and the  $\mathbf{S}^{(i)}$  becomes a symplectic matrix. We refer to this matrix form as form C and deal with it in Sec. VIII. The PRM is directly related to conductance in a quasi-one-dimensional electronic system. See Refs. [49–52] for the details.

Finally, in this paper we mainly treat some cases given by combinations of the three kinds of matrix form, i.e., A, B, and C, and two kinds of symbolization rules, i.e., types 1 and 2. (See Table I.)

### III. MODIFIED BERNOULLI MAP

In this section we briefly review the modified Bernoulli map and the statistical properties of the sequence. The map is

$$X_{i+1} = \begin{cases} X_i + 2^{B-1}(1-2b)X_i^B + b & (0 \leq X_i < 1/2) \\ X_i - 2^{B-1}(1-2b)(1-X_i)^B + b & (1/2 \leq X_i \leq 1), \end{cases} \quad (3.1)$$

where  $B$  is a bifurcation parameter that controls the correlation of the sequence.  $b$  is the deterministic perturbation, which is set as  $b = 10^{-12}$  only for  $B \geq 2$  in this paper. For numerical simulations  $b$  is used in order to overcome the difficulty that comes from nonstationarity. Stationarity is recovered by perturbation although the essential property remains invariant for a long time  $i < i_b$ , where  $i_b = (B-1)^{-1}(2b)^{(1-B)/B}$  [43]. Moreover, the sequence  $\{X_i\}$  can be symbolized by the following rule:

$$0 \leq X_i < 1/2 \rightarrow Y_i = -\frac{\epsilon}{2},$$

$$1/2 \leq X_i < 1 \rightarrow Y_i = \frac{\epsilon}{2}, \quad (3.2)$$

where the  $\epsilon$  is the strength of the fluctuation.

Another symbolic sequence is given by the following rule:

$$\begin{aligned} 0 \leq X_i < 1/2 &\rightarrow Y_i = \epsilon, \\ 1/2 \leq X_i < 1 &\rightarrow Y_i = 0. \end{aligned} \quad (3.3)$$

It is analytically shown that the correlation function of the symbolic sequence  $\{Y_i\}$  decreases as a power law for large  $n$  [44],

$$\langle Y_{n+1} Y_n \rangle \sim n^{-(2-B)/(B-1)}. \quad (3.4)$$

It is worth noting that when  $B < 2$  a normalizable stationary distribution (invariant measure) exists; on the other hand, when  $B \geq 2$  the sequence becomes nonstationary and a normalizable measure does not exist when  $b = 0$  [44]. This property of the sequence strongly affects the convergence of the Lyapunov exponents for the system. As we will mention in Sec. IV, we numerically judged the converged Lyapunov exponents even for the nonstationary region [42]. However, we restrict our numerical computation within  $B \leq 2.5$ , because it is difficult for large values of  $B$  to detect the convergent Lyapunov exponents. See Ref. [42] for more details of the convergence. We confirmed that the mean value and variance of the sequence we used in this paper are the same regardless of the parameter  $B$  even in the nonstationary region.

It was shown that the result does not depend qualitatively on the difference between  $\{X_i\}$  and  $\{Y_i\}$  in form A in our previous report [42]. We mainly use symbolic sequences that take only two values, 0 or  $\epsilon$  (type 1) and  $-\epsilon/2$  or  $\epsilon/2$  (type 2). When we use PRMs with form A and the symbolization rule of type 1, we refer to it as case A1. In a similar way, we use case B2 when matrix form B and the symbolization rule of type 2 are used.

In the case of form A, we generate the sequence of matrix elements as  $\{\omega_{jj+1}^{(n)} = Y_n, n = 1, 2, \dots\}$ , by the sequence of the modified Bernoulli map  $\{Y_n\}$  [43–45], where the different initial conditions of the map are used for each of  $N$  independent elements of an initial matrix  $\mathbf{H}^{(0)}$ . In the case of form B,  $N(N+1)/2$  independent matrix elements of the symmetric matrix  $\mathbf{H}^{(n)}$  are generated by  $\{\mathbf{H}_{ij}^{(n)} = \mathbf{H}_{ij}^{(n)} = Y_n, n = 1, 2, \dots\}$ , where the initial conditions are independent of  $i$  and  $j$ . In the case of form C, the  $N$  independent matrix elements are generated by  $\{V_{nj} = Y_n, n = 1, 2, \dots\}$ , where the initial conditions are independent of  $j$ .

### IV. LYAPUNOV EXPONENTS

In this section we give a definition of Lyapunov exponents that is used in Secs. V and VI, and also give local Lyapunov exponents, which are used in Sec. VII. We define local Lyapunov exponents  $\{[\lambda_i]_\tau, i = 1, \dots, 2N\}$  for a finite time interval  $\tau (= m \delta t)$  by means of the time evolution of eigenvalues of the real symmetric symplectic matrix

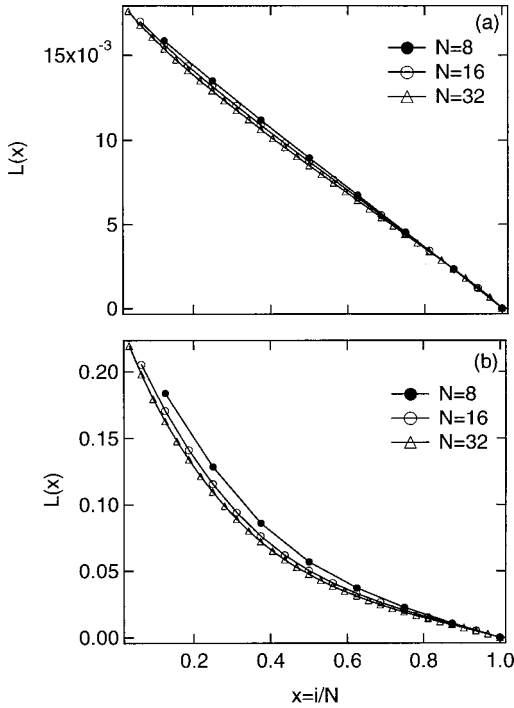


FIG. 1. Lyapunov spectra for matrix dimensions  $N = 8, 16, 32$  in (a) case A1 and (b) case A2 with  $\delta t = 1$  and  $\epsilon = 0.05$ .

$C_\tau = \mathbf{Z}(0)^\dagger \mathbf{P}(\tau)^\dagger \mathbf{P}(\tau) \mathbf{Z}(0)$  as follows:

$$[\lambda_i]_\tau = \frac{1}{2\tau} [\log \sigma_i(C_\tau)], \quad i = 1, \dots, 2N, \quad (4.1)$$

where  $\sigma_i(\cdot)$  denotes the  $i$ th eigenvalue. We set the exponents in decreasing order.

Instead of the Gram-Schmidt orthogonalization (GSO) method, we used the Householder QR-based method in order to calculate the Lyapunov exponents, which is better in accuracy and speed of numerical calculation than the GSO method [53,54]. We also got local Lyapunov exponents by direct calculation of the singular values of the matrix products.

## V. LYAPUNOV SPECTRA

In this section, we investigate the Lyapunov exponents  $L(x) = \lambda_i$  and the scaled Lyapunov exponents  $L_S(x) = \lambda_i / \lambda_1$  as a function of  $x (= i/N)$  for cases A1 and A2. We restrict our numerical computation within the case  $B \leq 2.5$ , because it is difficult to detect numerically convergent Lyapunov exponents for large values of  $B$ . (See Refs. [47,42].) We confirmed that the form of the Lyapunov spectra for  $N = 16$  is almost the same as for the larger dimensional matrix ( $N = 32$ ) in Fig. 1. Accordingly, we mainly use  $N = 16$  in order to reduce the computation time. The convergence of the Lyapunov exponents as a function of time  $m$  has been numerically confirmed for matrices in all cases we investigated.

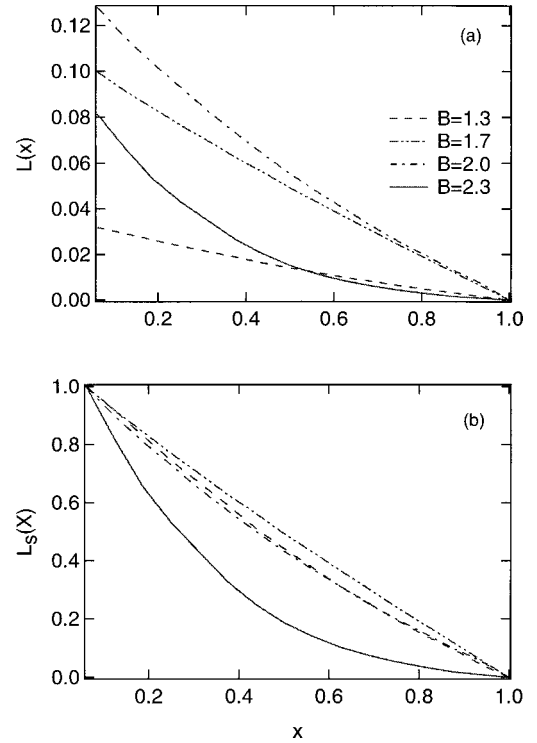


FIG. 2. (a) Lyapunov spectra  $L(x) = \lambda_i$  and (b) scaled Lyapunov spectra  $L_S(x) = \lambda_i / \lambda_1$  as a function of  $x = i/N$  in case A1 for some  $B$ 's with  $\delta t = 0.01$  and  $\epsilon = 5$ .

### A. Case A1

Recall that in the RMA without correlation the scaled Lyapunov spectra show the form  $L_S(x) = 1 - x$  in some models [28]. Figure 2 shows Lyapunov spectra  $L(x)$  and scaled Lyapunov spectra for various parameters  $B$  at  $\epsilon = 5$  and  $\delta t = 0.01$  in case A1. It follows that the effect of the correlation appears in the shape of the Lyapunov spectrum. It is shown in Fig. 2(b) that the shape of the spectrum gradually deviates from the linear form  $L_S(x) \sim 1 - x$  with increasing correlation. In the stationary region ( $B < 2$ ), the form of the Lyapunov spectrum does not greatly depend on the strength of the correlation and it is approximately linear, especially around  $x \sim 1$ . As  $B$  increases all of the Lyapunov exponents increase. This behavior means that the correlation enhances all of the indices of instability. Similar phenomena concerning the MLE have been observed in a one-dimensional disordered system with correlated diagonal disorder [16].

Moreover, in the nonstationary region ( $B \geq 2$ ) the MLE  $\lambda_1$  increases with increase of the correlation parameter  $B$ . On the other hand, the smaller Lyapunov exponents  $\lambda_{N-1}, \lambda_{N-2}, \dots$ , with values near zero ( $\lambda_i \sim 0$ ), begin to decrease when  $B$  becomes relatively large (beyond 2). The change of shape of  $L(x)$  with increasing  $B$  is quite interesting. It seems that the correlation does not make all of the Lyapunov exponents smaller monotonically, and allows the smaller Lyapunov exponents in the vicinity of zero decrease and approach zero.

### B. Case A2

Figure 3 shows Lyapunov spectra  $L(x)$  and scaled Lyapunov spectra  $L_S(x)$  for various parameters  $B$  at fixed

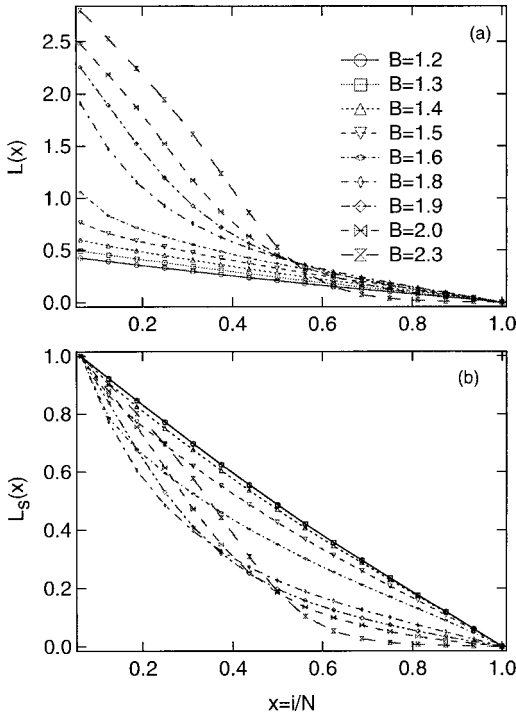


FIG. 3. (a) Lyapunov spectra  $L(x) = \lambda_i$  and (b) scaled Lyapunov spectra  $L_S(x) = \lambda_i/\lambda_1$  as a function of  $x = i/N$  in case A2 for some  $B$ 's with  $\delta t = 0.01$  and  $\epsilon = 5$ .

strength of the fluctuation  $\epsilon = 5$  and  $\delta t = 0.01$  in case A2. In the region  $1 < B < 3/2$  the functional forms of the scaled Lyapunov spectra are almost the same, and similar to that observed in the RMA, i.e., linear in  $x$ , independent of the correlation of the sequence. On the other hand, in the region  $B > 3/2$  and in the nonstationary region ( $B \geq 2$ ) the functional form of the scaled Lyapunov spectra has a characteristic form depending on  $B$ , and the form gradually approaches a hyperbolic function with increase of the correlation strength  $B$ .

### C. Summary

In the stationary region, the enhancement of all the Lyapunov exponents is related to the correlation of the sequence. A deviation from linear behavior around  $\lambda_1$  has been reported in some dynamical systems with strong correlation. Unfortunately, we are not able to give an analytical result for the correlation-enhanced instability observed in cases A1 and A2.

The behavior of the positive and smallest Lyapunov exponent observed for the nonstationary region in cases A1 and A2 is very important when we consider this phenomenon in the context of a dynamical system with correlation. It suggests that a few variables contribute to the instability on a short time scale, and the others yield a very slow dynamics. We confirmed that in cases B1 and B2 similar results to cases A1 and A2 could be obtained.

Moreover, when we consider the Lyapunov spectra from the point of view of the localization problem, the phenomena are also interesting. The positive and smallest Lyapunov exponent determines the localization length in a disordered sys-

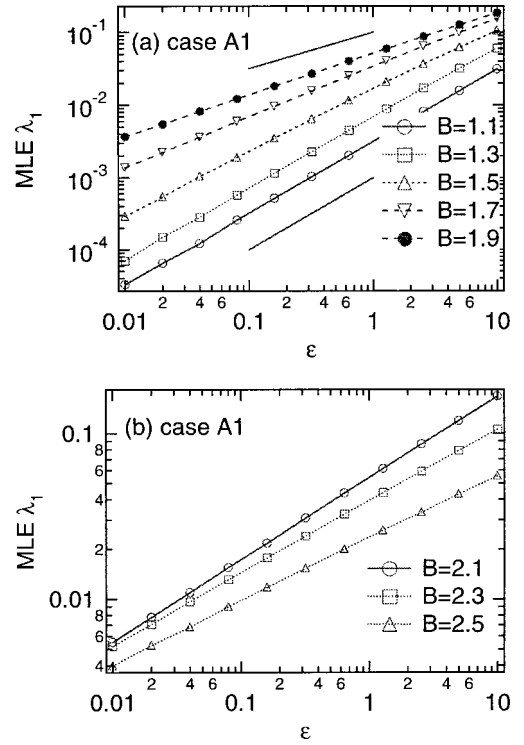


FIG. 4. Log-log plot of the fluctuation strength dependence of the MLE  $\lambda_1(\epsilon)$  for some  $B$ 's in case A1 with  $\delta t = 0.01$ . The lines denote  $\lambda_1 \propto \epsilon^1$  and  $\lambda_1 \propto \epsilon^{1/2}$ .

tem. We reconsider the correlation effect on the localization length in Secs. VIII and IX. We can expect that one important perspective on interesting phenomena can be obtained in analyzing the evolution of the Lyapunov vectors.

## VI. SCALING FORM OF THE MLE

In this section we present the  $\epsilon$  dependence of the MLE  $\lambda_1(\epsilon)$  in the cases A1 and A2. In the RMA, the scaling form

$$\lambda_1(\epsilon) \sim \epsilon^\beta \quad (6.1)$$

with  $\beta = 2/3$  for  $\langle \omega_{ii+1} \rangle \neq 0$  and  $\beta = 1/2$  for  $\langle \omega_{ii+1} \rangle = 0$ , where  $\langle \dots \rangle$  means the average of i.i.d. variables, has been derived by some analytical methods [11,12,3].

### A. Case A1

The  $\epsilon$  dependence of the MLE for case A1 with  $\delta t = 0.01$  is shown in Fig. 4. We compare the results for the  $\delta$ -correlated case with those obtained from the modified Bernoulli map. When  $B = 1.1$  a clear scaling rule,  $\lambda_1 \propto \epsilon^1$ , can be observed. The slope of the  $\epsilon$  dependence decreases and approaches one-half as  $B$  increases. As a result, a similar scaling law to Eq. (6.1) with  $1/2 \leq \beta \leq 1$  is observed for  $B$  in the stationary region  $B < 2$ . It is also found that the  $\epsilon$  dependence gradually deviates from linear behavior and shows decreasing slope in the relatively large  $\epsilon$  region.

On the other hand, in the nonstationary region ( $B > 2$ ) the MLE  $\lambda_1(\epsilon)$  shows a different type of scaling  $\lambda_1(\epsilon) \sim \epsilon^\beta$ , in which the slope  $\beta$  gradually decreases and simultaneously

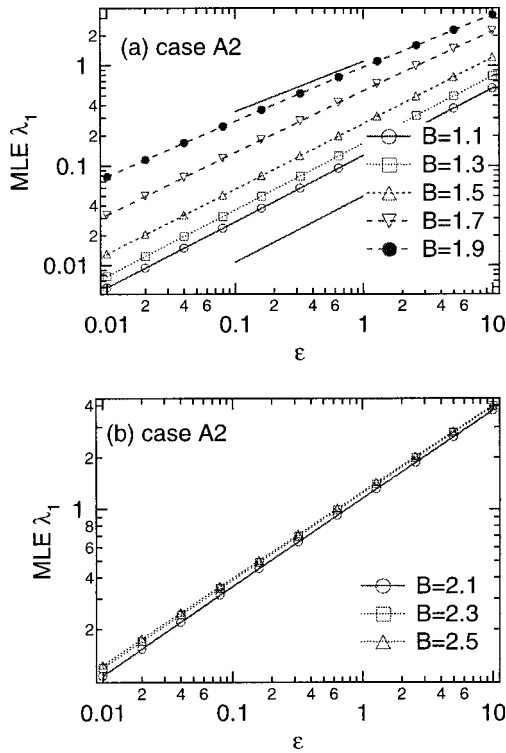


FIG. 5. Log-log plot of the fluctuation strength dependence of the MLE  $\lambda_1(\epsilon)$  for some  $B$ 's in case A2 with  $\delta t = 0.01$ . The lines denote  $\lambda_1 \propto \epsilon^{2/3}$  and  $\lambda_1 \propto \epsilon^{1/2}$ .

the value of the MLE decreases for increasing  $B$ .

We can guess that the order of the MLE with  $B$  will be changed at small  $\epsilon$ , based on extrapolation of the scaling form in Fig. 4(b). It is worth noting that we can say that correlation enhances the instability only at relatively small values of  $\epsilon$ .

### B. Case A2

Figure 5 shows the fluctuation strength dependence of the MLE  $\lambda_1(\epsilon)$  in case A2 with  $\delta t = 0.01$ . As seen in case A1, it seems that on a logarithmic scale the  $\epsilon$  dependence shows good linear approximation and the slope slightly decreases as the correlation increases in the stationary region ( $B < 2$ ). As we might expect, on a logarithmic scale, a clear scaling law  $\lambda \sim \epsilon^{2/3}$ , which is similar to the case of the RMA, is observed for  $B = 1.1$ . This is a different feature of the case A2 from the case A1. Note that the sequence generated by  $B = 1.0$ , i.e., the Bernoulli map, has the same KS entropy mathematically as random coin tossing [46].

As a result, we observed clear scaling laws  $\lambda_1(\epsilon) \sim \epsilon^\beta$  depending on the correlation, in which the exponent  $\beta$  takes intermediate values between  $2/3$  and  $1/2$  in the stationary region. On the other hand, in the nonstationary region ( $B > 2$ ) the correlation does not affect the scaling form of the MLE  $\lambda_1$  strongly. In case B2 almost the same phenomena as in case A2 were observed as the correlation increases.

## VII. DISTRIBUTION OF LOCAL LYAPUNOV EXPONENTS

When a product of a finite number  $m$  of matrices is considered, the corresponding local Lyapunov exponents are

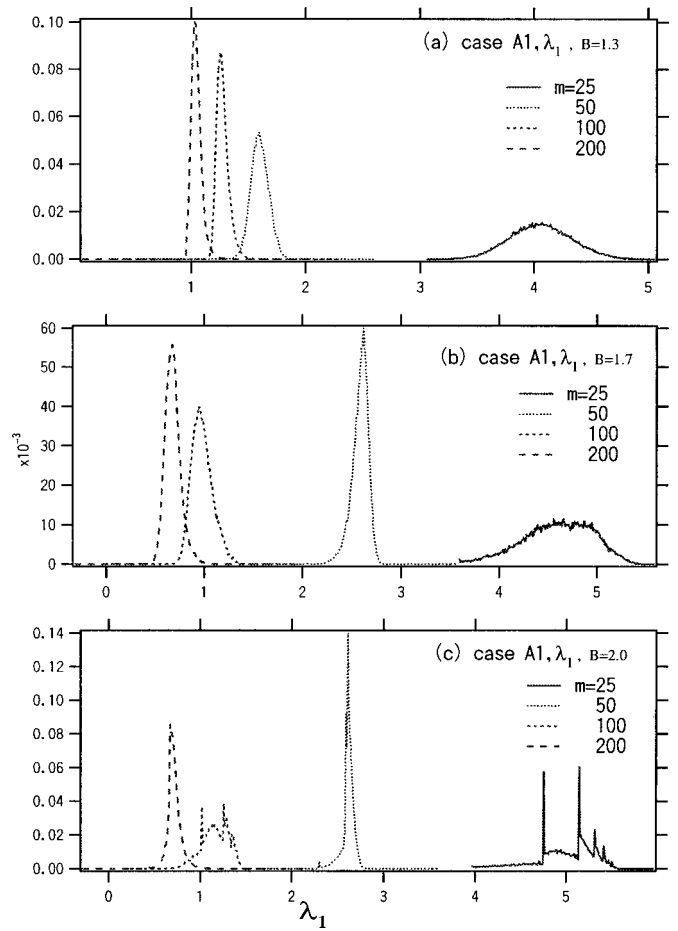


FIG. 6. Probability distribution of local maximal Lyapunov exponents  $P([\lambda_1]_\tau)$  for some typical  $\tau$  ( $= \delta t m$ ) at (a)  $B = 1.3$ , (b)  $B = 1.7$ , and (c)  $B = 2.0$  in case A1 with  $\delta t = 0.01$  and  $\epsilon = 5$ .

distributed over the initial conditions. In this section, we investigate the probability distribution of local Lyapunov exponents for cases A1, A2, B1, and B2. We pay particular attention to the change of location of peaks and the convergence properties of the probability distribution. Falcioni *et al.* investigated the convergence of the probability distribution of the MLE in a high-dimensional symplectic map [55]. The coupling strength  $\epsilon$  dependence of the convergence with respect to  $m$  was reported.

### A. Case A1 and B1: Maximal Lyapunov exponent

In Figs. 6 and 7, probability distributions of local MLEs  $P([\lambda_1]_\tau)$  for some typical  $\tau$  [ $= \delta t m$ , where the  $m$  is the interval used to decide the local Lyapunov exponents, i.e.,  $m$  is the number of matrices in Eq. (2.1)], are shown for (a)  $B = 1.3$ , (b)  $B = 1.7$ , and (c)  $B = 2.0$  for cases A1 and B1, respectively. The ensemble size is 40 000, i.e., the probability distributions are made from an ensemble of 40 000 different initial conditions for each independent matrix element.

It is found that in the case of  $B = 1.3$  the form of the distribution is Gaussian independent of the value  $m$ . Note that in the case of random symplectic matrix products the probability distribution form for Lyapunov exponents  $\lambda_i$  has

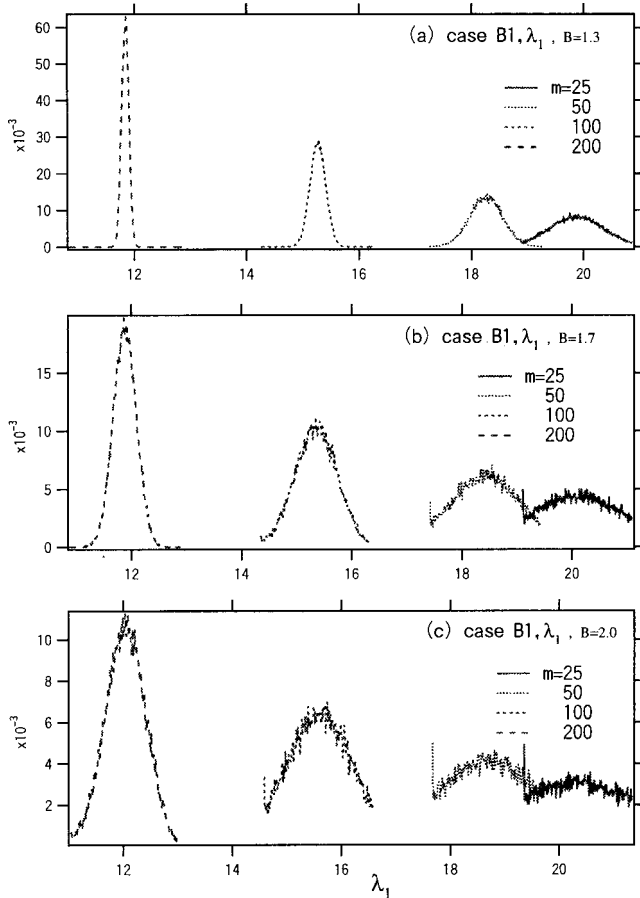


FIG. 7. Probability distribution of local maximal Lyapunov exponents  $P([\lambda_1]_\tau)$  for some typical  $\tau$  ( $=\delta t m$ ) at (a)  $B=1.3$ , (b)  $B=1.7$ , and (c)  $B=2.0$  in case B1 with  $\delta t=0.001$  and  $\epsilon=5$ .

been analytically derived by some methods, such as perturbation [8], functional equations [56,57], and so on [24]. Owing to the CLT the fluctuation is generally well approximated by a Gaussian distribution in  $\delta$ -correlated PRMs. As a result, the convergence of the probability distribution obeys  $\sigma \sim m^{-1/2}$  with respect to  $m$ .

As  $B=1.3$  is relatively small, the statistical properties of the sequence are similar to those of  $\delta$ -correlated case. On the other hand, as we can see in Fig. 6(c) and Fig. 7(c) for larger values of  $B$  the distribution shows anomalous structure especially at small  $m$ . Some sharp peaks exist in the probability distribution with a broad peak in the center, and as  $m$  increases the sharp peak is absorbed in the broad peak and disappears. The origin of the sharp peak at small  $\lambda_1$  is due to products of identical matrices generated by the almost periodic sequence.

In Fig. 8 the  $m$  dependence of the standard deviation  $\sigma$  of the distribution is shown in order to estimate the speed of convergence of the distribution with regard to increase of  $m$ . The distribution converges with increasing  $m$  with a drift of the mean values  $\langle \lambda_1 \rangle_m$ . The speed of convergence of the  $m$ -dependent mean value becomes slower as  $B$  becomes larger.

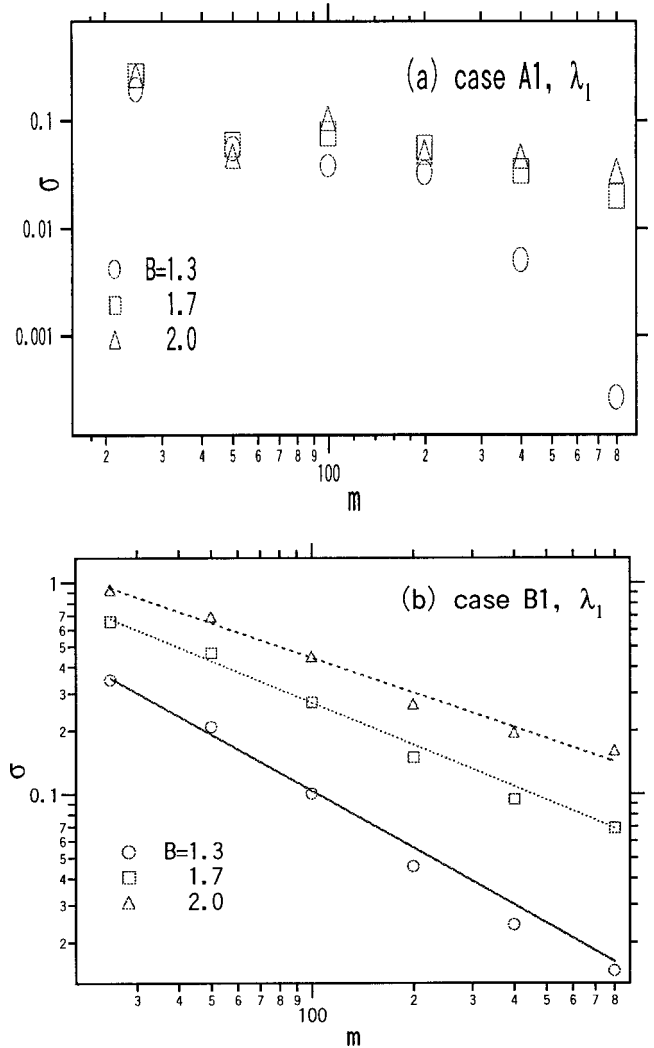


FIG. 8. Log-log plot of standard deviation of the probability distribution as a function of time interval  $m$  in case (a) A1 and (b) B1. The lines are the linear least-squares fits for the  $m$  dependence.

### B. Case A2 and B2: Maximal Lyapunov exponent

In Fig. 9, the distributions of local MLEs  $P([\lambda_1]_\tau)$  for  $B=1.2$ ,  $B=1.5$ , and  $B=1.8$  in the case A2 are shown. The spiky peaks on the broad distribution at small  $m$  are due to the small ensemble size. When we pay attention to the global feature of the distribution form, the peak structure and the convergence properties of the probability distribution are similar to the ones obtained in cases A1 and B1. In particular, for case  $B=1.9$  a multipeak structure is clearly observed, and the shape of the probability distributions is different from Gaussian. But in order to confirm the details of the functional form of the distribution, a much larger ensemble is necessary in cases of larger parameter  $B$ . We observed that the distribution of the local MLEs in case B2 is almost Gaussian even for  $B=1.8$ .

Figure 10 shows the  $m$  dependence of the standard deviation of the probability distribution of MLEs in cases A2 and B2. The qualitative structure of the convergence is similar to that for A1 and B1. We try to characterize the slow conver-



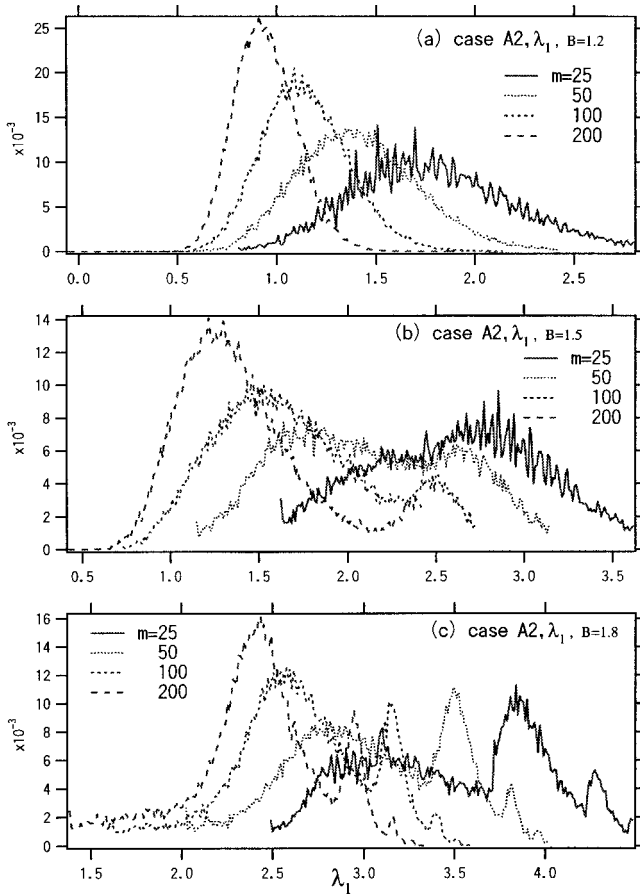


FIG. 9. Probability distribution of local maximal Lyapunov exponents  $P([\lambda_1]_\tau)$  for some typical  $\tau$  ( $=\delta t m$ ) at (a)  $B=1.2$ , (b)  $B=1.5$ , and (c)  $B=1.8$  in case A2 with  $\delta t=0.01$  and  $\epsilon=5$ .

gence for large  $B$ . In Fig. 11 we show the convergence index  $\alpha_i(B)$  of the distribution of the local Lyapunov exponents, which is defined by the change of the standard deviation,

$$\sigma = \sqrt{\langle (\Delta \lambda_i)^2 \rangle_\Omega} \sim m^{-\alpha_i(B)}, \quad (7.1)$$

where  $\langle \dots \rangle_\Omega$  means the ensemble average, and the  $i$ th exponent  $\alpha_i$  corresponds to distribution of the  $i$ th local Lyapunov exponent  $\lambda_i$ . We used linear least-squares fitting for the data in Figs. 8 and 10. The index  $\alpha_1$  decreases with increase of the parameter  $B$ . The slow convergence in the distribution of the MLEs is based on anomalous statistical properties of the modified Bernoulli map. In the next subsection we investigate the other Lyapunov exponents in cases A2 and B2.

### C. Case A2 and B2: The other Lyapunov exponents

In Figs. 12 and 13, distributions of the local seventh and fifteenth largest Lyapunov exponents  $P([\lambda_7]_\tau)$  and  $P([\lambda_{15}]_\tau)$  for case A2 are shown. The distributions are not smooth, and in some cases the singular-peak structure is clearly observed. In particular, the narrow peak on the left side of the main broad peak grows gradually with increase of  $m$  in case A2 with  $B=1.5$ . On the other hand, Fig. 13(c) shows that the sharp peaks on the right side of the broad

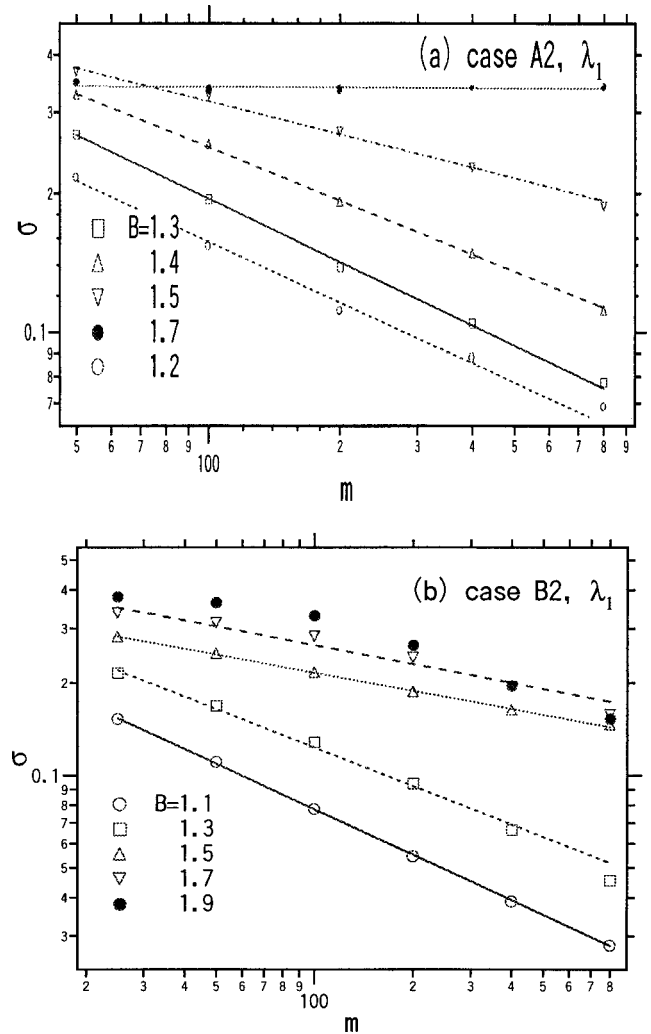


FIG. 10. Log-log plot of standard deviation of the probability distribution as a function of time interval  $m$  in case (a) A2 and (b) B2. The lines are the linear least-squares fits for the  $m$  dependence.

peak of the distribution  $P([\lambda_{15}]_\tau)$  gradually disappear with increase of the  $m$ . In case A2 the whole structure of the convergence is similar to that for case A1. Figure 14 shows the probability distribution of the local fifteenth largest Lyapunov exponents  $P([\lambda_{15}]_\tau)$  for case B2. Unlike the other cases, a double-peak structure is not observed even for large values of  $B$  at small  $m$ . Figure 14(c) shows that in the case  $B=2.3$  the probability distribution shape does not change for increase of  $m$ .

Figures 15 and 16 show the  $m$  dependence of the standard deviation of the distribution of some Lyapunov exponents in some cases. A linear  $m$  dependence is observed for some cases in case B2. In Fig. 17 the indices  $\alpha_7(B)$  and  $\alpha_{15}(B)$  of the convergence as a functions  $B$ , estimated by least-squares fitting using Eq. (7.1) for the standard deviation of the distribution, are shown. The case of  $B=1.1$  obeys the CLT, i.e.,  $\alpha \approx 0.5$  approximately. As  $B$  increases  $\alpha$  decreases because of the correlation effect. Accordingly, the correlation strongly affects the convergence properties of the probability distribution function of not only local MLEs but also the other local Lyapunov exponents.

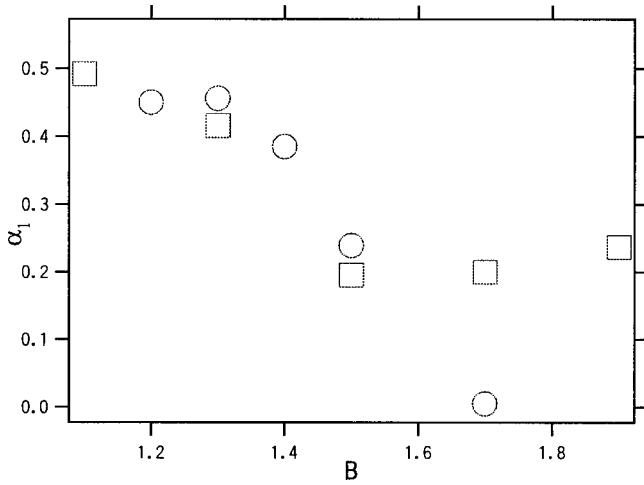


FIG. 11. The index  $\alpha_1$  as a function of  $B$ , estimated by the convergence of the standard deviation in cases A1 (open circles) and B2 (open squares).

We recall that similar features for the probability distribution of Lyapunov exponents exist in other systems. When we investigated the distribution of Lyapunov exponents in  $2 \times 2$  PRMs with correlation in the problem of a one-dimensional disordered system, a double-peak structure

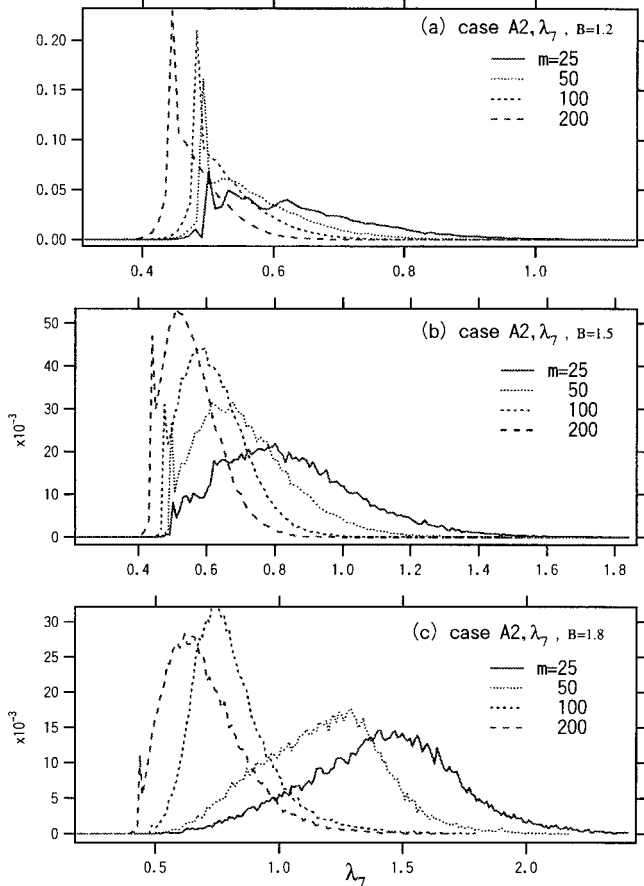


FIG. 12. Probability distribution of local maximal Lyapunov exponents  $P([\lambda_\gamma]_\tau)$  for some typical  $\tau$  ( $=\delta t m$ ) at (a)  $B=1.2$ , (b)  $B=1.5$ , and (c)  $B=1.8$  in case A2 with  $\delta t=0.01$  and  $\epsilon=5$ .

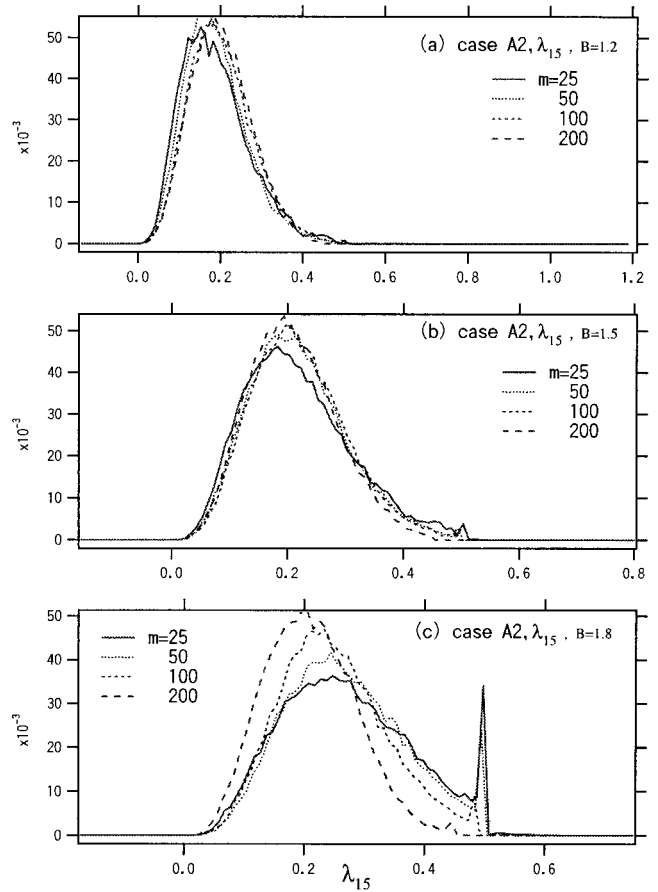


FIG. 13. Probability distribution of local maximal Lyapunov exponents  $P([\lambda_{15}]_\tau)$  for some typical  $\tau$  ( $=\delta t m$ ) at (a)  $B=1.2$ , (b)  $B=1.5$ , and (c)  $B=1.8$  in case A2 with  $\delta t=0.01$  and  $\epsilon=5$ .

could be clearly observed in the distribution, and the distribution form had slow convergence for  $3/2 \leq B < 2$  [36].

In a  $\delta$ -correlated disordered system, the differential equation obeyed by the probability distribution function of conductance has been derived [8,59,60]. As a result, the convergence of the distribution obeys a standard CLT for the limit of large system size. However, correlation effects obeying power-law decay in the Lyapunov exponents and the scaling property of  $\lambda_i(\epsilon)$  are still open problems.

### VIII. CASE C2

In this section, we show some numerical results for the Lyapunov spectra, scaling form of the MLE, and convergence properties of the distribution of local MLEs in case C2.

Figure 18 shows the Lyapunov spectra  $L(x)$  for some  $B$ 's in case C2 at  $\epsilon=0.01$  and  $E=0$ . The energy of the electron corresponds to the band center of the two-dimensional system. In the figure a  $\delta$ -correlated case with uniform distribution in  $[-0.01, 0.01]$  is added as a reference. In comparison with the  $\delta$ -correlated case all of the Lyapunov exponents decrease. The structure of the  $B$  dependence is similar to that in the case A2 except that some Lyapunov exponents are zero regardless of the strength of the correlation. The second largest Lyapunov exponent  $\lambda_2$  determines the localization

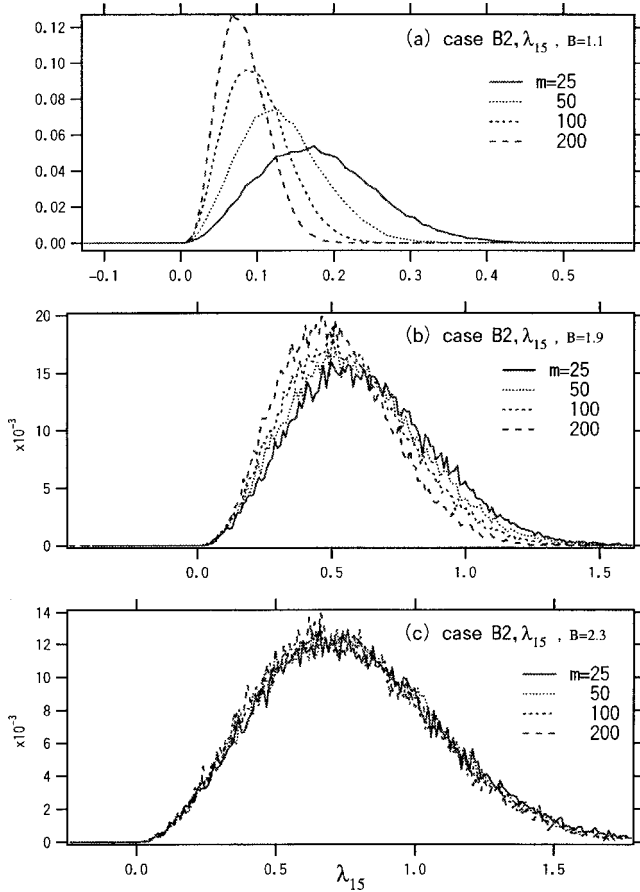


FIG. 14. Probability distribution of local maximal Lyapunov exponents  $P([\lambda_{15}]_\tau)$  for some typical  $\tau (= \delta t m)$  at (a)  $B=1.1$ , (b)  $B=1.9$ , and (c)  $B=2.3$  in case B2 with  $\delta t=0.01$  and  $\epsilon=5$ .

length as shown in Fig. 18 because it does not vanish. Roughly speaking, it seems that  $\lambda_2$  decreases as the correlation strength increases.

Figure 19 shows the fluctuation strength dependence of the MLE  $\lambda_1(\epsilon)$  for some  $B$ 's in case C2. As  $\epsilon$  increases, the MLE changes from some positive value to another positive value at some critical value  $\epsilon_c$  that depends on the correlation parameter  $B$ . The larger  $\epsilon_c$  becomes, the larger is parameter  $B$ . In other words, this system has a transition. The relation between the existence of the transition and the localization problem is very interesting. The localization property is strongly related to a singularity in the density of states [16]. Accordingly, to make it clearer, further investigations are necessary in a wider parameter range. The results will be reported elsewhere [58].

## IX. SUMMARY AND DISCUSSION

We have systematically investigated the Lyapunov spectra, scaling form of the MLE, and convergence properties of the probability distribution of local MLEs in correlated PRMs with long-range correlation, which is generated by a modified Bernoulli map. The results we obtained in the present investigation are summarized as follows.

(1) In cases A1 and A2, the forms of the Lyapunov spec-

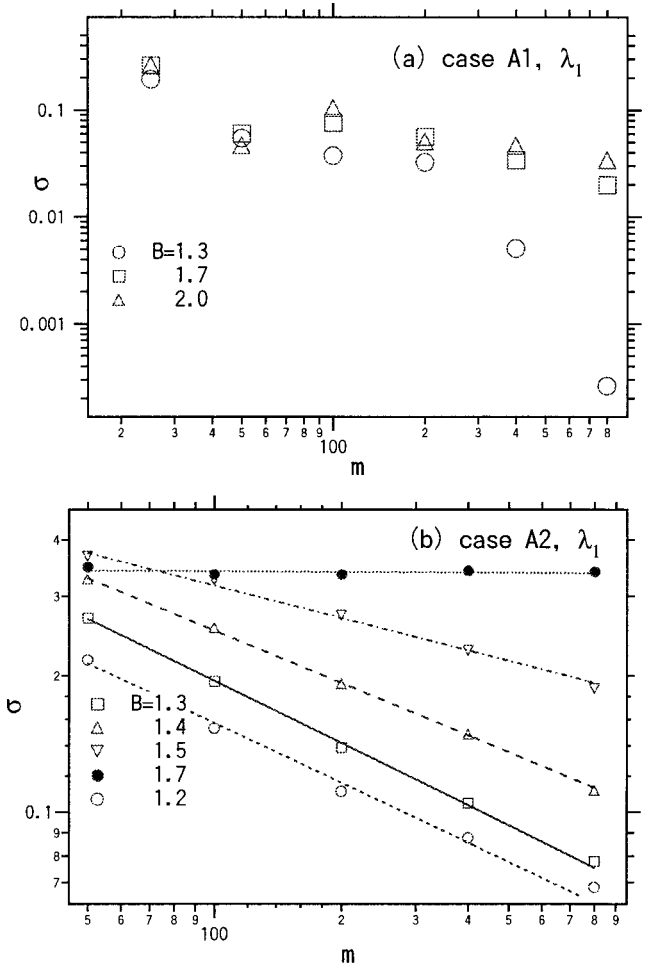


FIG. 15. Log-log plot of standard deviation of the probability distribution (a)  $P([\lambda_7]_\tau)$  and (b)  $P([\lambda_{15}]_\tau)$  as a function of time interval  $m$  in case A2.

tra for the correlated cases are different from that obtained from  $\delta$ -correlated random matrices. In the stationary region ( $B < 2$ ) all of the Lyapunov exponents  $\{\lambda_i\}$  increase with increase of the correlation parameter  $B$ . On the other hand, the value of the smaller Lyapunov exponents around  $x \sim 1$  begins to decrease when  $B$  becomes relatively large (beyond 2) in the nonstationary region ( $B \geq 2$ ).

(2) In case A1 the slope of the  $\epsilon$  dependence decreases from unity and approaches one-half as  $B$  increases. As a result, similar scaling laws to Eq. (6.1) with  $1/2 \leq \beta \leq 1$  are observed for any  $B$  in the stationary region  $B < 2$ .

(3) In case A2, the  $\epsilon$  dependence  $\lambda_1(\epsilon)$  also shows a good linear approximation on the logarithmic scale and the slope decreases as the correlation increases in the stationary region ( $B < 2$ ). In the case of  $B \geq 2$ , a clear scaling law with  $\beta = 1$  is observed, which is different from those derived from the RMA.

(4) In cases A1 and A2, for larger values of  $B$  the probability distributions show multipeak structures especially at small  $m$ , where a sharp peak corresponds to the almost periodic sequence generated by the map. The probability distributions converge with increasing  $m$  with drift of the mean

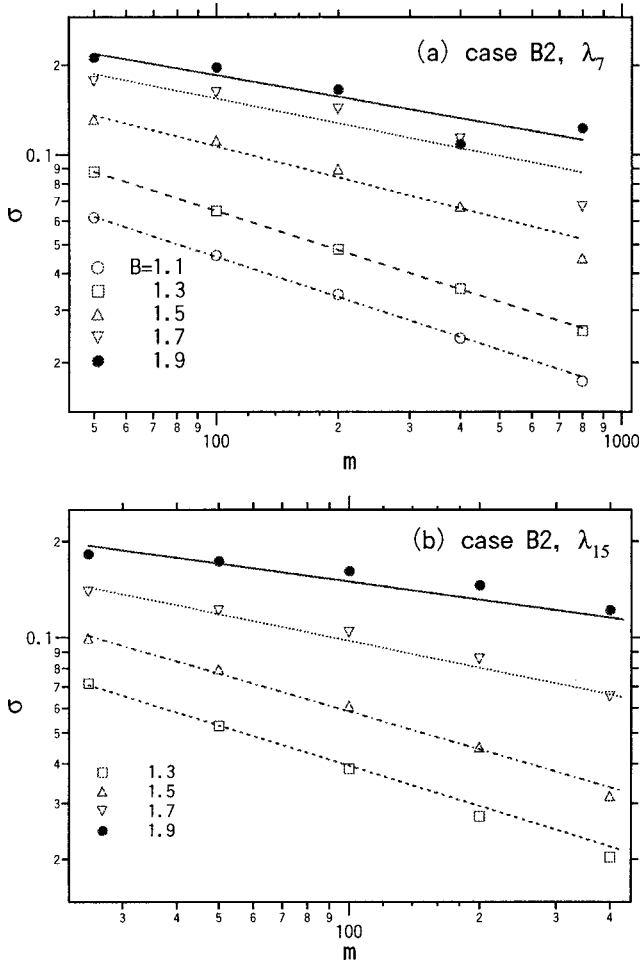


FIG. 16. Log-log plot of standard deviation of the probability distribution (a)  $P([\lambda_7]_\tau)$  and (b)  $P([\lambda_{15}]_\tau)$  as a function of time interval  $m$  in case B2. The lines are the linear least-squares fits for the  $m$  dependence.

value. Qualitatively, the speed of convergence becomes slower as  $B$  becomes larger.

(5) In cases A2 and B2, the distribution of local maximal Lyapunov exponents  $P([\lambda_1]_\tau)$  shows the multipeak structure also. The shape of the distributions is different from Gaussian for large  $B$ . The convergence index  $\alpha_i(B)$ , which characterizes the slow convergence of the probability distribution, becomes small with increase of  $B$ .

(6) In cases A2 and B2, the distribution forms for the local seventh and fifteenth largest Lyapunov exponents  $P([\lambda_7]_\tau)$  and  $P([\lambda_{15}]_\tau)$  show slow convergence, i.e.,  $\alpha_7$  and  $\alpha_{15}$  are less than one-half, which would correspond to the  $\delta$ -correlated case. Correlation strongly affects the convergence properties of the distribution functions of not only the local MLEs but also the other local Lyapunov exponents.

(7) In other cases, the Lyapunov spectra, scaling form of the MLE, and convergence properties of the probability distribution of local MLEs have also been investigated, and some similar features to those of cases A1 and A2 have been observed.

We would like to mention some physical meaning in the results. We observed deviation from the linear form in

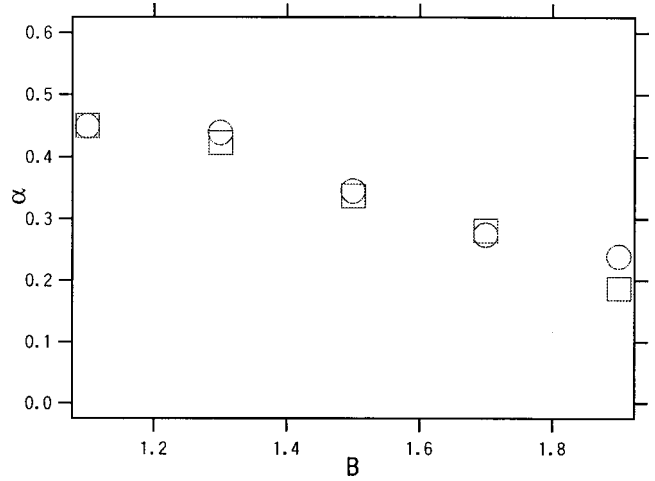


FIG. 17. The index  $\alpha_7$  (open circles) and  $\alpha_{15}$  (open squares) as a function of  $B$ , estimated from convergence of the standard deviation in case B2.

Lyapunov spectra  $L(x)$  and  $L_5(x)$  and squeezing of the Lyapunov spectra near  $x \sim 0$  as the correlation of the sequence increases. If we express the situation with words in a dynamical system, this suggests that a few variables contribute to chaotic motion on a short time scale, while all the others yield a very slow dynamics. In other words, the first chaotic behavior is confined to a low-dimensional manifold.

There is controversy about exponential localization in two-dimensional disordered systems [61]. The simple scaling theory concludes that in the two-dimensional disordered system almost all of the eigenstates are exponentially localized [62]. However, some experimental and theoretical reports suggest the existence of nonexponentially localized states when the strength of disorder is small [63,64]. The relation between the existence of the ‘‘pseudo mobility edge,’’ which

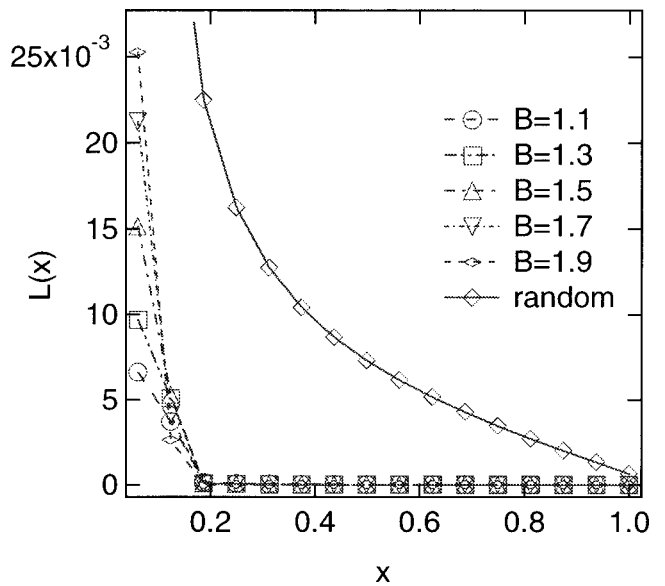


FIG. 18. Lyapunov spectra  $L(x) = \lambda_i$  as a function of  $x = i/N$  in case C2 for some  $B$ 's with  $\epsilon = 0.01$ . A  $\delta$ -correlated case with uniform distribution in  $[-0.01, 0.01]$  is added as a reference.

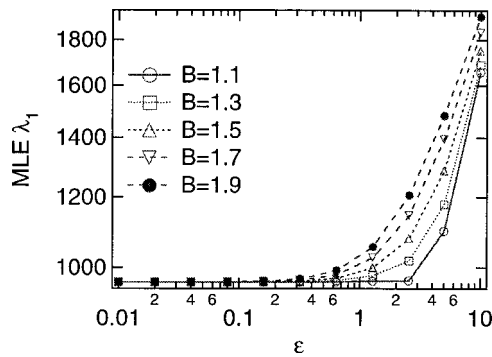


FIG. 19. Log-log plot of the fluctuation strength dependence of the MLE  $\lambda_1(\epsilon)$  for some  $B$ 's in case C2 with  $\epsilon=0.01$ .

divides power-law localizations from exponential ones, and the Lyapunov spectra and the  $\epsilon$  dependence of the MLE in case C2 is very interesting. Even in disordered electronic system correlations are often present and may play an important role. It can be said that we confirmed the effects of the spatial correlation on localization length of the wave function.

The positive and smallest Lyapunov exponents correspond to the inverse of the localization length. The correlation of the matrix sequence, in general, works to enhance delocalization. As expected, it was found that the presence of correlation between impurities in the Anderson model leads to an enhancement of delocalization at the band center energy. To make clearer the localization property, further systematic investigations are necessary for larger random matrices.

Unfortunately, at the present stage we have not succeeded

in analytical derivation of the interesting phenomena caused by correlation. We can construct other models for the PRM with correlation by using a sequence  $\{X_i\}$  generated by a modified Bernoulli map. First we prepare two kinds of symplectic matrices  $\mathbf{A}$  and  $\mathbf{B}$ , for which the matrix elements are set as in forms  $\mathbf{A}$ ,  $\mathbf{B}$ , or  $\mathbf{C}$ . The correlated products of the matrices  $\Pi_{i=1}^m M_i$  are created by the rule

$$\begin{aligned} 0 \leq X_i < 1/2 &\rightarrow M_i = \mathbf{A}, \\ 1/2 \leq X_i < 1 &\rightarrow M_i = \mathbf{B}. \end{aligned} \quad (9.1)$$

Then analytical treatment for the Lyapunov exponents will be easier than for those used in this paper, because the sequence can be well approximated by a renewal process [43]. We will try to do this elsewhere [58].

Further systematic investigation of the relation between the Lyapunov exponents and matrix form and/or correlation in the products is necessary too. Moreover, there are other interesting problems concerning the Lyapunov exponents of the products of matrices with correlation, such as the effect of correlation between matrix elements on Lyapunov exponents, which has not been included in the present study. Many problems are open for future study.

#### ACKNOWLEDGMENTS

We would like to thank Dr. Y. Y. Yamaguchi and Professor T. Konishi for discussions. We also thank Professor M. Goda for useful comments and encouragement. H.Y. would like to thank Professor M. Wilkinson for his hospitality during a stay in the University of Strathclyde. Numerical computation in this work was carried out on the computer system of the National Institute of Materials and Chemical Research.

- 
- [1] P. Bougerol and J. Lacroix, *Products of Random Matrices with Applications to Schrodinger Operators* (Birkhauser, Boston, 1985), and references therein.
- [2] *Random Matrices and Their Applications*, edited by J. E. Kasten and C. M. Newman (American Mathematical Society, Providence, RI, 1986), and references therein.
- [3] A. Crisanti, G. Paladin, and A. Vulpiani, *Products of Random Matrices in Statistical Physics* (Springer-Verlag, Berlin, 1993), and references therein.
- [4] H. Matsuda and K. Ishii, *Prog. Theor. Phys.* **45**, 56 (1970).
- [5] K. Ishii, *Prog. Theor. Phys.* **53**, 77 (1973).
- [6] T. M. Nieuwenhuizen and J. M. Luck, *J. Stat. Phys.* **41**, 745 (1985).
- [7] P. Erdos and C. R. Herndon, *Adv. Phys.* **31**, 429 (1981).
- [8] P. A. Mello, P. Pereyra, and K. Kumar, *Ann. Phys. (N.Y.)* **181**, 290 (1988).
- [9] B. M. MacCoy and T. T. Wu, *Phys. Rev.* **176**, 631 (1968).
- [10] A. Crisanti, G. Paladin, M. Serva, and A. Vulpiani, *Phys. Rev. E* **49**, R953 (1994).
- [11] G. Benettin, *Physica D* **13**, 211 (1984).
- [12] G. Paladin and A. Vulpiani, *J. Phys. A* **19**, 1881 (1986).
- [13] R. Livi, A. Politi, and S. Ruffo, *J. Phys. A* **19**, 2033 (1986).
- [14] R. Livi, A. Politi, S. Ruffo, and A. Vulpiani, *J. Stat. Phys.* **46**, 147 (1987).
- [15] G. Paladin and A. Vulpiani, *Phys. Rep.* **156**, 147 (1987).
- [16] A. Crisanti, G. Paladin, and A. Vulpiani, *Phys. Rev. A* **39**, 6491 (1989).
- [17] H. A. Posch and W. G. Hoover, *Phys. Rev. A* **38**, 473 (1988).
- [18] G. Seeley and T. Keyes, *J. Chem. Phys.* **91**, 5581 (1989).
- [19] S. Sastry, *Phys. Rev. Lett.* **76**, 3738 (1996).
- [20] J. Cook and B. Derrida, *J. Stat. Phys.* **61**, 961 (1990).
- [21] H. Furstenberg, *Trans. Am. Math. Soc.* **108**, 377 (1963).
- [22] V. I. Oseledec, *Trans. Moscow Math. Soc.* **19**, 197 (1968).
- [23] V. N. Tutubalin, *Theor. Probab. Appl.* **13**, 65 (1968).
- [24] A. D. Virster, *Theor. Probab. Appl.* **15**, 667 (1970).
- [25] H. Furstenberg and H. Kesten, *Ann. Math. Stat.* **31**, 457 (1960).
- [26] A. J. O'Connor, *Commun. Math. Phys.* **45**, 63 (1975).
- [27] P. R. Mello, *J. Math. Phys.* **27**, 2876 (1986).
- [28] C. M. Newman, *Commun. Math. Phys.* **103**, 121 (1986).
- [29] J. P. Eckmann and C. E. Wayne, *J. Stat. Phys.* **50**, 853 (1988).
- [30] G. J. Kissel, *Phys. Rev. A* **44**, 1008 (1991).
- [31] K. Fukamachi, *Europhys. Lett.* **26**, 26 (1994).
- [32] T. Okabe and H. Yamada, *Chaos, Solitons and Fractals* **9**, 1755 (1998).
- [33] T. Konishi and K. Kaneko, *J. Phys. A* **25**, 6283 (1992).
- [34] K. Kaneko and T. Konishi, *Physica D* **71**, 146 (1994).

- [35] C. Amitrano and R. S. Berry, Phys. Rev. Lett. **68**, 729 (1992); Phys. Rev. E **47**, 3158 (1993).
- [36] H. Yamada, M. Goda, and Y. Aizawa, J. Phys.: Condens. Matter **3**, 10 043 (1991).
- [37] F. Cecconi and A. Vulpiani, Phys. Lett. A **201**, 326 (1995).
- [38] M. J. de Oliver and A. Petri, Phys. Rev. E **53**, 2960 (1996).
- [39] M. Goda, Prog. Theor. Phys. **62**, 608 (1979).
- [40] A. Lahiri and L. Nilsson, Chem. Phys. Lett. **311**, 459 (1999).
- [41] Y. Y. Yamaguchi, J. Phys. A **31**, 195 (1998).
- [42] T. Okabe and H. Yamada, Prog. Theor. Phys. Suppl. **138**, 615 (2000).
- [43] Y. Aizawa, Prog. Theor. Phys. **72**, 659 (1984).
- [44] Y. Aizawa, C. Murakami, and T. Kohyama, Prog. Theor. Phys. Suppl. **79**, 96 (1984).
- [45] K. Tanaka and Y. Aizawa, Prog. Theor. Phys. **90**, 547 (1993).
- [46] A. J. Lichtenberg and M. A. Lieberman, *Regular and Chaotic Dynamics* (Springer-Verlag, New York, 1992).
- [47] T. Okabe and H. Yamada, Int. J. Mod. Phys. B **12**, 901 (1998); Mod. Phys. Lett. B **12**, 615 (1998).
- [48] H.-O. Canmesin and Y. Fan, J. Phys. A **23**, 3613 (1990).
- [49] J. L. Pichard and G. Andre, Europhys. Lett. **2**, 477 (1986).
- [50] B. Derrida, K. Mecheri, and J. L. Pichard, J. Phys. (Paris) **48**, 733 (1987).
- [51] P. Markos and B. Kramer, Philos. Mag. B **68**, 357 (1993).
- [52] P. Markos, J. Stat. Phys. **70**, 899 (1993).
- [53] K. Geist, U. Parlitz, and W. Lauterborn, Prog. Theor. Phys. **83**, 875 (1990).
- [54] H. F. Bremen, F. E. Udawadia, and W. Proskurowski, Physica D **101**, 1 (1997).
- [55] M. Falcioni, U. M. B. Marconi, and A. Vulpiani, Phys. Rev. A **44**, 2263 (1991).
- [56] A. Gamba and I. V. Kolokolov, J. Stat. Phys. **85**, 489 (1996).
- [57] X. R. Wang, J. Phys. A **29**, 3053 (1996).
- [58] T. Okabe and H. Yamada (unpublished).
- [59] C. W. J. Beenakker, Rev. Mod. Phys. **69**, 731 (1997).
- [60] T. Guhr, A. M. Groeling, and H. A. Weidenmueller, Phys. Rep. **299**, 189 (1998).
- [61] M. Goda, M. Ya. Azbel, and H. Yamada, Int. J. Mod. Phys. B **13**, 2705 (1999).
- [62] E. Abrahams, P. W. Anderson, D. C. Licciadello, and T. V. Ramakrishnan, Phys. Rev. Lett. **42**, 673 (1979).
- [63] M. Ya. Azbel, Phys. Rev. B **26**, 4735 (1982).
- [64] N. F. Mott and M. Kaveh, Adv. Phys. **34**, 329 (1985).